Correlation between surface physicochemical properties and the release of iron from stainless steel AISI 304 in biological media

Yolanda Hedberg [a,*], Maria-Elisa Karlsson [a], Eva Blomberg [a,b],
Inger Odnevall Wallinder [a], Jonas Hedberg [a]

[a] KTH Royal Institute of Technology, Dept. Chemistry, Div. Surface and Corrosion Science, Drottning Kristinas väg 51, SE-100 44 Stockholm, Sweden
[b] SP Technical Research Institute of Sweden, Chemistry, Materials and Surfaces, P.O. Box 5607, SE-114 86 Stockholm, Sweden

ABSTRACT

Stainless steel is widely used in biological environments, for example as implant material or in food applications, where adsorption-controlled ligand-induced metal release is of importance from a corrosion, health, and food safety perspective. The objective of this study was to elucidate potential correlations between surface energy and wettability of stainless steel surfaces and the release of iron in complexing biological media. This was accomplished by studying changes in surface energies calculated from contact angle measurements, surface oxide composition (X-ray photoelectron spectroscopy), and released iron (graphite furnace atomic absorption spectroscopy) for stainless steel grade AISI 304 immersed in fluids containing bovine serum albumin or citric acid, and non-complexing fluids such as NaCl, NaOH, and HNO_3. It was shown that the surface wettability and polar surface energy components were all influenced by adventitious atmospheric carbon (surface contamination of low molecular weight), rather than differences in surface oxide composition in non-complexing solutions. Adsorption of both BSA and citrate, which resulted in ligand-induced metal release, strongly influenced the wettability and the surface energy, and correlated well with the measured released amount of iron.

1. Introduction

1.1. The surface of stainless steel is changed due to corrosion processes

Stainless steel is widely used in biological environments, for example as implant materials [1] or in food contact applications [2,3]. Such environments inevitably result in the adsorption of proteins that can significantly influence the surface oxide characteristics and enhance the release of metals, even if stainless steel is in its passive state (not actively corroding) and maintains a high corrosion resistance [4]. The surface oxide ("passive film") of all stainless steel grades is mainly composed of iron(III) and chromium(III) oxides and is typically 2–5 nm thick in most acidic and neutral environments at room temperature with no applied potential [4–7]. The relative proportion of chromium (Cr) to iron (Fe) in the surface oxide is not necessarily altered upon contact with neutral non-complexing aqueous solutions [4,7]. It is, however, strongly affected (enhanced proportion of Cr) in acidic, complexing (chelating), and/or protein-containing solutions, such as citric acid/citrate [6,8,9], nitric acid [6], sulfuric acid [7,10], and solutions containing bovine serum albumin (BSA) [4].

1.2. Corrosion and metal release are influenced by ligand-induced processes in complexing solutions

The surface oxide of stainless steel is in complexing environments exposed to different ligands (complexing agents) such as citrate and proteins. This induces ligand adsorption, complexation with a surface oxide/hydroxide metal atom, and the possible detachment of the ligand–metal complex from the surface oxide (rate limiting step) [11]. Ligand-induced metal release is hence adsorption-dependent [12,13], but also dependent on pH [12], stability constants of surface complexes [9,14], and on other parameters such as temperature [15]. Depending on the environment, the metal release from stainless steel is also influenced by other processes including active corrosion and protonation [4,11,14]. The dynamic exchange of proteins between the surface and the solution is important for the metal release process, and depends on various factors including protein concentration and agitation [16].

1.3. Electrostatic (EL), electrodynamic (LW), and polar (AB) interactions are important for surface adsorption of solution species

Surface adsorption is influenced by the surface charge of stainless steel and of adsorbed species [17], which results in electrostatic (EL) forces (repelling or attractive) [18]. Non-polar (electrodynamic, or Lifshitz-van der Waals – LW), and polar (electron–donor, electron–acceptor, or Lewis acid–base – AB) interactions are both important for any surface adsorption [17–19]. These properties can be determined via contact angle measurements using liquids of different and known surface energy components [18]. Dehydration of water at the surface and changes in protein conformation where the driving force is a net gain in entropy, are important in the case of BSA adsorption. This process takes place even if the polarity is the same as the stainless steel surface [20,21].

1.4. The zeta potential of stainless steel is negative at neutral pH

The surface charge is important for the adsorption of proteins (especially for small, hard proteins), since one of the driving forces for protein adsorption on stainless steel is electrostatic [17,20,21]. The zeta potential of massive stainless steel is commonly reported as negative at neutral pH and the isoelectric point (IEP) was identified between pH 3 and 5 [4,21–24]. Even significantly higher IEPs, between 6 and 8.5, have been reported for stainless steel particles [25,26] and massive sheet of stainless steel (predicted data) [27,28]. More positive IEPs of nano- and micron-sized stainless steel particles compared with massive sheet may be explained by differences in surface oxide speciation (such as composition, thickness, crystallinity, phase distribution, and catalytic properties) [29–31]. No significant differences in IEP have been reported in the literature [32] for different pure metal particles and their corresponding bulk oxides. However, since all of these particles were treated in NaOH and HNO$_3$ prior to the measurements, this might have influenced the results. Reported IEPs of bulk oxides and hydroxides of iron and chromium vary between 4.5 and 8.5 [33,34]. This is higher compared with measurements for massive stainless steel surface oxides made of similar constituents. Somewhat lower IEPs have been reported for several metals and alloys (e.g. stainless steel) [23,35] with thin surface oxides (as compared with bulk oxides). The lower IEPs of metals could possibly be explained by a mirror effect of electrons at the metallic interface adjacent to the thin surface oxide [36,37].

1.5. Aim

The aim of this study was to elucidate the importance and connection between surface physicochemical characteristics including surface energy and wettability with the release of iron from stainless steel surfaces in complexing biological media. The study hypothesis was that BSA and citrate adsorption, which results in ligand-induced metal release, influence the surface energy of the stainless steel surface. This information on wettability and surface properties could provide further information about metal release mechanisms and link the surface biochemical aspects with corrosion and metal release processes.

Differences in surface energies calculated from contact angle measurements, surface oxide composition, and released iron from stainless steel grade AISI 304 immersed in complexing solutions containing bovine serum albumin or citric acid were studied. The influence of both polar and non-polar surface energies was studied in relation to metal release by using both the van Oss et al. [38,39] and the Della Volpe et al. [40] methods.

Table 1
Surface tension parameters (mJ/m^2) of the different liquids, using values from van Oss et al. [38,39] and Della Volpe et al. [40].

Liquid	Van Oss et al. (vOCG)				Della Volpe et al.			
	γ_{TOT}	γ_{LW}	γ^-	γ^+	γ_{TOT}	γ_{LW}	γ^-	γ^+
Water	72.8	21.8	25.5	25.5	72.8	26.2	11.2	48.5
Glycerol	64	34	57.4	3.92	63.5	35	27.8	7.33
Diiodomethane	50.8	50.8	0	0	50.8	50.8	0	0
Formamide	58	39	39.6	2.25	58.1	35.5	11.3	11.3

Table 2
Microstructure and bulk composition (wt.%) of the austenitic stainless steel grade AISI 304, based on supplier information.

Cr	Fe	Mn	Ni	Mo	C	P	Si	S
18.1	Balance	1.1	9.0	0.3	0.05	0.03	0.3	0.002

2. Materials and methods

2.1. Calculation of polar and non-polar surface energies and choice of methods

Based on the Young–Dupreé equation, the free surface energy of a solid material (γ_{TOT}) and its acid-base (γ^+ and γ^-) and Lifshitz-van der Waals (γ_{LW}) components of the surface free energy [38,39,41] are assumed to be additive according to Eq. (1) [41]:

$$\gamma_{TOT} = \gamma_{LW} + \sqrt{\gamma^+ \gamma^-} \qquad (1)$$

Contact angle measurements between a liquid of known properties and a surface can be used to calculate the free surface energy components by utilizing at least three liquids with different properties, and solving three equations of this type (2) [38,39]:

$$(1 + \cos\theta) = 2(\sqrt{\gamma_S^{LW}\gamma_L^{LW}} + \sqrt{\gamma_S^+\gamma_L^-} + \sqrt{\gamma_S^-\gamma_L^+}) \qquad (2)$$

Here, θ is the contact angle and S and L denote the solid and liquid phase, respectively. At least one of the liquids should be non-polar ($\gamma^+ = \gamma^- = 0$), giving the γ_{LW} component of the solid surface directly. However, there are conflicting opinions in the literature on how to perform these types of measurements and calculations. The method of van Oss et al. (vOCG) [38,39] has been criticized by Della Volpe et al. [40,42] for the choice of liquids used for contact angle measurements, selected values for their corresponding free energies, and the direct comparison between acid and basic properties. This will however not be discussed in detail in this paper. We therefore report surface energy values calculated using both the vOCG and the Della Volpe et al. methods to allow relative comparisons between the methods for differently treated surfaces. Water, formamide and glycerol, or water, formamide and diiodomethane combinations were selected to obtain well-conditioned sets of equations [40]. Surface tension parameters for the different liquids are given in Table 1.

A Matlab (version 7.8) program using a least-square method was used for solving non-linear equations for each liquid (Eq. (2)).

2.2. Exposure conditions and surface treatments

Stainless steel AISI 304 (Table 2) coupons approximately sized 1.0 cm × 1.0 cm × 0.1 cm and with a total surface area of 1.98–2.40 cm^2 were polished down to 0.25 μm (diamond paste) and ultrasonically cleaned between each grinding/polishing step for 3 min in acetone. The coupons were then ultrasonically cleaned in acetone and isopropyl alcohol for 7 min, dried with cold nitrogen gas, and positioned in a desiccator (room temperature) for 24 ± 1 h prior to exposure. The cleaning and aging procedure was selected to

enable comparison with literature data [4], and to allow the growth of a defined surface oxide. Contact angle measurements were made on 2–4 coupons, and X-ray photoelectron spectroscopy performed on 2 coupons directly after polishing and after aging. The other coupons were put in acid cleaned polypropylene centrifuge tubes to which 4 mL of the respective solution was added (surface area to solution volume ratio of $0.5 \, cm^{-1}$). Four individual coupons were exposed for each test condition, with one blank solution sample (no coupon added) exposed in parallel. Immersion was conducted at $37 \pm 0.5\,^{\circ}C$ (Stuart platform-rocker incubator, 25 cycles/min of bilinear shaking) in:

- 10 mM NaCl (0.584 g/L, Merck, initial pH 5.8), for 10 min (pH decreased to 5.1 ± 0.1) and 24 h (pH increased to 6.0 ± 0.1)
- citric acid (5.0 g/L, 99% purity, Sigma–Aldrich, initial pH 2.4), for 10 min (pH unchanged: 2.4), 1 h (pH decreased to 2.3 ± 0.007), 24 h (pH decreased to 2.1 ± 0.01), and 168 h (pH decreased to 2.3 ± 0.01)
- 10 mM NaCl containing 10 g/L bovine serum albumin (BSA, L: 120M1886 V, Sigma–Aldrich, initial pH 6.7 ± 0.5), denoted NaCl + BSA, for 10 min (pH decreased to 6.6 ± 0.1), 1 h (pH decreased to 5.3 ± 0.8), 24 h (pH decreased to 6.0 ± 0.3), and 168 h (pH was unchanged: 7.0 ± 0.02).

In addition, four coupons were exposed at $60 \pm 2\,^{\circ}C$ to 6 M HNO₃ (initial pH <0) for 1 h (pH <0), and to 2 M NaOH (initial pH of 13.0) for 2 h (pH unchanged: 13.0). Another four coupons were exposed to 6 M HNO₃ (as above), followed by measurement of contact angle. They were then cleaned according to the above procedure (acetone and isopropyl alcohol) and exposed to citric acid for 24 h (final pH 2.3 ± 0.03).

After exposure, all coupons were rinsed with ultrapure water (18.2 MΩ cm) for 5 s (if not denoted differently). Subsequently (<10 min), they were dried with cold nitrogen gas followed by immediate (<2 h) measurement of contact angle. To ensure accurate trace metal analysis of released iron from the stainless steel in solution all vessels and equipment were acid-cleaned in 10% HNO₃ for at least 24 h, rinsed four times in ultrapure water (18.2 MΩ cm), and dried in ambient laboratory air. All chemicals were of analytical grade (p.a.) or puriss p.a. grade (in the case of nitric acid used for solution sample acidification prior to atomic absorption spectroscopy analyses).

2.3. Contact angle measurements

Static contact angles were determined using a PG-X pocket goniometer (Fibro Systems AB, Sweden). To avoid cross-contamination between the investigated fluids, each fluid had a unique set of tubes and syringes. The contact angle was measured after a 3–20 s delay, and after another 5–15 s delay between each drop. Individual static contact angle measurements were performed twice for each coupon and fluid. Between two and five coupons were measured for each exposure condition. Contact angle data is presented as average values and standard deviation between all coupons for each exposure condition (between 4 and 10 single measurements), or for single coupons (2 single measurements), as indicated in figures and tables.

2.4. Metal release measurements

Graphite Furnace Atomic Absorption Spectroscopy (GF-AAS) using a Perkin Elmer AAnalyst 800 instrument was used to determine the amount of released iron in each acidified (65 vol% ultrapure HNO₃, pH <2) solution sample. The method by Vogelsang et al. [43] was used to determine the limit of detection (LOD), limit of identification (LOI), and limit of quantification (LOQ). The

calibration curve was based on calibration standards (in 1 vol% HNO₃) of 0, 5, 10, 25, 50, and 100 μg/L. The curve was linear up to 25 μg/L, and non-linear at higher concentrations (100 μg/L deviated −34% from the extrapolated linear curve). The non-linearity of the curve was accounted for by the instrument using a non-linear fitting curve through zero. The LOD, LOI, and LOQ were calculated based on the calibration points 5, 10, and 25 μg/L (in the linear range) by comparing the calibration signals with signals of spiked samples in each fluid. LOD values of 2.1, 0.5, and 0.5 μg/L Fe were determined in citric acid, in 10 mM NaCl, and in NaCl + BSA, respectively. The corresponding LOI numbers were 4.1, 1.0, and 1.0 μg/L Fe, respectively. The LOQ values were determined to be 6.0, 1.4, and 1.5 μg/L Fe in citric acid, in 10 mM NaCl, and in NaCl + BSA, respectively. The recoveries of 5, 10, and 25 μg/L spiked samples, which should not deviate more than 15% from 100%, were all between 94 and 107%. Since the acidified HNO₃ and NaOH solutions were similar to the calibration standard matrix, their LOD, LOI, and LOQ values were lower compared with the other solutions, <2.1, <4.1, and <6.0 μg/L Fe, respectively. Solution samples of HNO₃, NaOH, citric acid, and NaCl + BSA (two samples after 24 h, all samples after 168 h) were diluted 12.5 times to ensure that concentrations were within the calibration range. The blank values of all samples were positive and subtracted from the significantly higher solution sample values. The blank values were <1% of the sample values in NaCl, <1.7% in citric acid and HNO₃, and 24% after 10 min, 16% after 1 h, and <1.7% after 24 or 168 h in NaCl + BSA. Relatively high blank values (between 1.3 and 22 μg/L Fe) and their variation in the BSA contacting fluids were attributed to the iron content of BSA, as previously reported in Lundin et al. [44]. This influence was accounted for in average values and standard deviations using a background correction for Fe in BSA (see supporting information).

2.5. Surface oxide composition measurements

Surface compositional analysis was performed using X-ray photoelectron spectroscopy, XPS. Spectra were recorded using a Kratos AXIS UltraDLD X-ray photoelectron spectrometer (Kratos Analytical) using a monochromatic Al X-ray source (150 W) on areas of approximate size $700 \, \mu m \times 300 \, \mu m$. Wide spectra (survey scans) were run to identify elements present in the outermost surface oxide (information depth of a few nanometers). High resolution spectra (20 eV pass energy) were acquired for the main bulk compositional elements Cr 2p, Fe 2p, and O 1 s of each test coupon including carbon (C 1 s). Two readings were performed for each coupon, and duplicate coupons, resulting in four high resolution spectra in total investigated for each surface treatment. Peak positions were referenced to the C 1 s peak at 285.0 eV. The relative content of oxidized iron and chromium in the outermost surface oxide was determined and presented as their relative mass ratio, $Cr_{ox}/(Cr_{ox} + Fe_{ox})$. Based on the peak positions for oxidized Cr and Fe (Cr_{met}: 574.3 ± 0.1 eV, Cr_{ox}: 577.5 ± 1.1 eV, Fe_{met}: 707.1 ± 0.1 eV, Fe_{ox}: 710.8 ± 1.8 eV) and previous investigations [4,44], Cr was present in its trivalent oxidation state for all conditions and Fe was present in its trivalent or divalent oxidation states. No deconvolution of the Fe 2p peak was made to resolve the oxidation state of iron.

3. Results and discussion

3.1. Surface contamination is the main explanation for differences in wettability and polar components of the surface energy of stainless steel in non-complexing fluids

Fig. 1 shows static water contact angles, amounts of carbon in the outermost surface and amounts of oxidized chromium
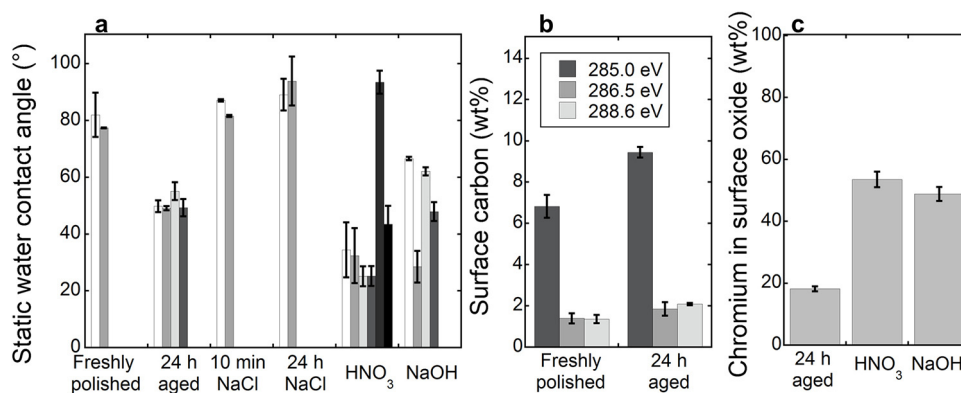
Fig. 1. Static contact angles and corresponding standard deviations for differently pre-treated stainless steel coupons of grade 304 at different surface areas of each coupon (a), amounts of surface carbon for two independent coupons (285.0 eV: C—C and C—H bonds [51,52]; 286.5 ± 0.2 eV: C—O, and C—N bonds [51,52]; 288.6 ± 0.1 eV: O—C=O bonds [52]) measured by means of XPS (b), and the relative percentage of oxidized chromium in the surface oxide (oxidized Fe and Cr) measured by means of XPS at four different surface areas of two independent coupons for different pre-treatments (c). The average and standard deviation of single coupons (measured 1–2 times at 2 locations) (a) or two independent coupons, measured at 2 different locations twice, are shown (b and c).

in the surface oxide (as determined by XPS), for selected exposures/treatments. The 304 stainless steel coupons showed large variations in water contact angles, in agreement with literature findings (between <10 and 126°) depending on surface treatment [3,45–49]. No clear correlation was observed between the contact angles, Fig. 1a, and the oxide composition, Fig. 1c. We therefore postulate that observed variations among, or within, different surface treatments, Fig. 1a, were mainly related to the extent of surface contamination (represented by the total amount of surface carbon). This is supported by literature findings on reduced water contact angles with reduced surface contaminations [48,49], and the observation that no relation was evident with changes in surface oxide composition [48,49]. A metal surface that is essentially free of contamination would result in a totally wetted surface [50]. Surface contamination can be derived from cleaning solvents (acetone or isopropyl alcohol) and from adventitious atmospheric carbon, and is mainly characterized by C—C and C—H bonds (285.0 eV), Fig. 1b.

Surface energy values are compiled in Table 3, based on static contact angle measurements of water, formamide, and diiodomethane, and calculated using the vOCG and the Della Volpe et al. methods (see Section 2 for details). Analogous calculations using the combination of water, glycerol and diiodomethane showed similar trends (see Table S1). The methods by vOCG [38,39] and Della Volpe et al. [40] differ mainly in the polar component γ^- (see Table 3) and reveal similar trends between the different treatments/exposures. Calculated γ values according to the vOCG method are in agreement with literature findings for stainless steels [45,46,53,54]. The results revealed generally higher γ^- values compared with γ^+, and γ_{LW} values of approximately 40 mJ/m². The relatively higher γ^- values are expected due to the negative zeta potential (low IEP) of stainless steel [55]. The extent of 40 mJ/m² for the non-polar component γ_{LW} of the surface energy is similar to many other compounds, e.g. various proteins [56] or stainless steel cleaned in different ways [49].

Exposure to 10 mM NaCl for 10 min resulted in a less polar surface, as indicated by a significantly reduced γ^- value ($p < 0.05$, as determined by a student t-test of unpaired data and unequal variance) compared to the freshly polished and aged coupons. It could not be concluded whether this difference, not observed after 24 h in the same medium, was due to additional surface contamination, or an exposure effect. The amount of released iron during the exposures (see Table 3) correlated with the enrichment of chromium in the surface oxide as in Fig. 1. The correlation between released iron and chromium enrichment of the surface oxide is well-documented for stainless steel in its passive state [31,57–59]. It is explained by

a preferential release of iron compared with chromium that results in a more passive chromium-rich surface oxide over time. No clear correlation was observed between the Fe/Cr ratio in the surface oxide and the calculated γ^- values for any conditions. This is in agreement with some literature findings [49], but in contrast with other findings for γ^- values exceeding 25 mJ/m² [60]. Surface treatments with HNO₃ or NaOH both resulted in relatively high amounts of released iron, Table 3, a pronounced enrichment of chromium in the surface oxide, Fig. 1c, and relatively low observed water contact angles and high calculated γ^- values. The latter is most probably related to a reduced surface contamination.

No significant differences in static contact angles or chromium enrichment in the surface oxide were observed among samples treated for 24 h in citric acid, or passivated by HNO₃, or after HNO₃ passivation and 24 h exposure in citric acid in sequence, Fig. 2. This may be connected to relatively low amounts of surface contamination due to relatively rapid surface processes. Such processes could be electrochemical corrosion (oxidation of metal) and ligand-induced chemical or electrochemical surface oxide dissolution [11], and adsorption of citrate, further discussed below. The HNO₃ passivation pre-treatment, which results in the formation of a stable passive surface oxide of high electrochemical barrier properties [6,61], caused, as expected, significantly lower released amounts of iron into citric acid, Fig. 2c. It could be argued that a lack of correlation between surface composition and wettability/surface energy is due to the fact that the chromium oxidation state remained trivalent throughout all investigations. Previous investigations have however not been able to show any relationship between the surface composition of stainless steel and its wettability properties, even when changing the chromium oxidation state at the surface from trivalent to hexavalent chromium by means of oxygen plasma treatment [49].

The results emphasize that the extent of surface contamination (atmospheric adventitious carbon and possibly adsorbed solvents from surface cleaning [46,62]) largely influences measured static contact angles and hence calculated surface energies of polished, aged surfaces of stainless steel and when exposed in non-complexing media.

### 3.2. Metal release and wettability correlate due to adsorption of BSA and citrate

Fig. 3 displays results on iron release, contact angles, and calculated γ^- components for stainless steel immersed in NaCl + BSA. While the amount of released iron was similar compared with

Table 3
Static contact angles of water, and calculated surface energy values (mJ/m^2) based on contact angle measurements with water, formamide, and diiodomethane using the van Oss et al. [38,39] and Della Volpe et al. [40] methods, and released amounts of iron per surface area in each fluid.[a]

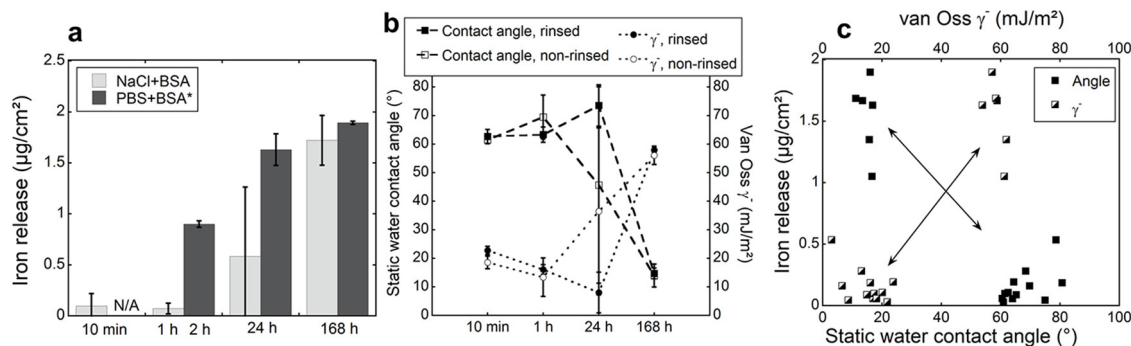|	Water contact angles	van Oss γ_{LW}	van Oss γ^-	van Oss γ^+	Della Volpe γ_{LW}	Della Volpe γ^-	Della Volpe γ^+	Released iron (μg/cm^2)
Freshly polished	80 ± 3.3	38 ± 0.34	7.2 ± 1.7	0 ± 0	39 ± 0.50	2.1 ± 0.53	0 ± 0	–
24 h aged	51 ± 2.9	40 ± 1.0	33 ± 3.0	0 ± 0	39 ± 1.1	13 ± 1.4	0 ± 0	–
10 min NaCl	84 ± 3.9	39 ± 3.9	4.4 ± 1.0	0 ± 0	40 ± 3.5	1.1 ± 0.32	0 ± 0	0.27 ± 0.080
24 h NaCl	92 ± 3.4	40 ± 0.95	39 ± 20	0 ± 0	40 ± 0.82	15 ± 7.8	0 ± 0	0.25 ± 0.12
1 h HNO$_3$	42 ± 26	43 ± 2.2	43 ± 23	0.13 ± 0.32	42 ± 3.0	19 ± 9.7	0.24 ± 0.58	2.4 ± 0.66
2 h NaOH	51 ± 17	41 ± 3.2	31 ± 19	0.048 ± 0.073	41 ± 3.0	13 ± 7.4	0 ± 0	0.96 ± 0.099

[a] The water contact angles and surface energy values are shown as average values and standard deviations of 2–4 independent samples, 2 different locations on each sample, and 1–2 measurements on the same location, i.e. 4–16 single measurements. Released iron is shown as the average value and standard deviation of three independent samples, which were measured three times, i.e. 9 single measurements.
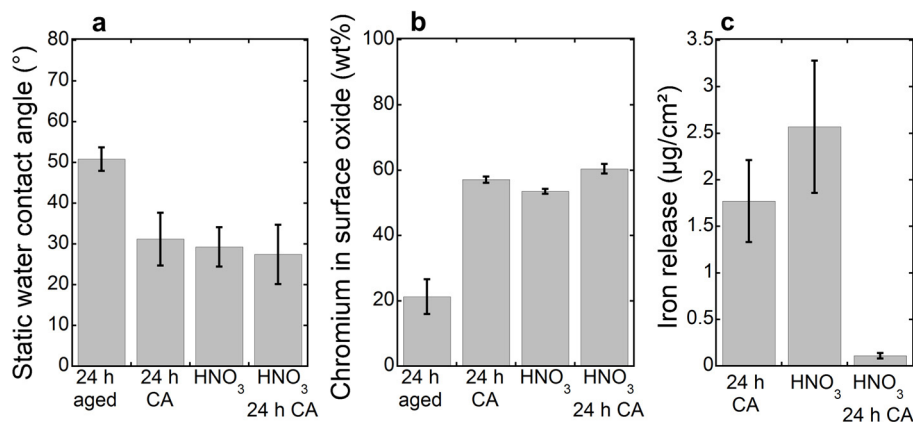
Fig. 2. Static water contact angle (a), relative amount of oxidized chromium in surface oxide (oxidized Fe + Cr) measured by means of XPS (b), and amount of iron released into solution measured by means of GF-AAS (c), for non-exposed polished and aged (24 h) stainless steel 304 coupons, 24 h citric acid, 1 h HNO$_3$, and subsequently 24 h citric acid (pre-treated in 1 h HNO$_3$) (c.f. material and methods). The error bars show the standard deviation between four independent samples. CA denotes citric acid.

literature findings in phosphate buffered saline and 10 g/L BSA (PBS + BSA, otherwise similar conditions) [4] after 168 h of exposure, it was significantly lower for the shorter exposure time periods between 10 min and 24 h, Fig. 3a. Increased metal release in solutions of increased BSA concentration has previously been attributed to structural changes of the adsorbed BSA layer [4,16,63]. The adsorption of BSA at high solution concentrations (10 g/L) is fast due to a high mass transport flux [63]. Thus, significantly reduced contact angles after 24 h of exposure (Fig. 3b) may be explained by structural changes of the adsorbed BSA layer. Literature reports of water contact angles for a film of pure, hydrated BSA, or adsorbed on a passive metal (Ti), showed very low contact angles (<13°) [56,64]. As the BSA molecules are more shielded due to counter ions in solutions of higher ionic strength [21], the repulsive force between BSA molecules and the surface is reduced. From this follows a random orientation of adsorbed BSA in solutions of higher ionic strength. Lower released amounts of iron for the short exposure time period in NaCl + BSA of lower ionic strength compared with the PBS + BSA solution may hence be explained by initially less interaction between the stainless steel surface and the BSA due to higher repulsive forces. Increased interaction resulted in higher amounts of released iron, either indirectly (facilitated chemical or electrochemical dissolution of surface oxide or the metallic interface due to weakened metal–oxygen bonds, deaeration, or reduced pH) or directly by the release of protein–metal complexes. The latter case is possible for agitated solutions of relatively high protein
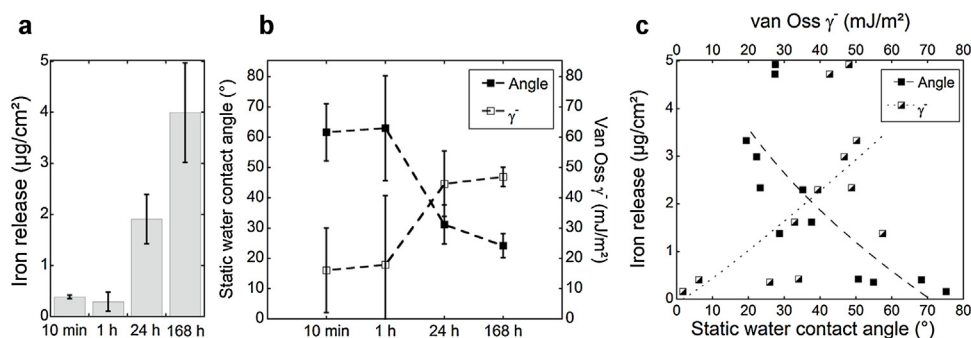

Fig. 3. Iron released into solution measured by means of GF-AAS (a), static water contact angles, and corresponding van Oss et al. γ^- values (based on water, formamide, and diiodomethane) (b), and their correlation for individual coupons (c) of stainless steel 304 exposed to NaCl + BSA for 10 min, 1, 24, and 168 h, respectively. *Literature data [4] for identical exposure conditions in phosphate buffered saline (8.77 g/L NaCl, 1.28 g/L Na$_2$HPO$_4$, 1.36 g/L KH$_2$PO$_4$, pH 7.2–7.4) and 10 g/L NaCl (PBS + BSA) after 2, 24, and 168 h, is included for comparison. N/A – no literature data available. The dotted lines are only guidance for the eye. Error bars: (a) background corrected standard deviation between 4 and 6 independent samples (c.f. experimental and supporting information), (b) standard deviation between 2 or 3 independent coupons.

Table 4

Static contact angles of water, and surface energy values (mJ/m^2) calculated from contact angles of water, formamide, and diiodomethane, using the method of van Oss et al. [38,39] and Della Volpe [40].[a]

	Water contact angles	van Oss γ_{LW}	van Oss γ^-	van Oss γ^+	Della Volpe γ_{LW}	Della Volpe γ^-	Della Volpe γ^+	Released iron (μg/cm^2)
Freshly polished	80 ± 3.3	38 ± 0.34	7.2 ± 1.7	0 ± 0	39 ± 0.50	2.1 ± 0.53	0 ± 0	–
24 h aged	51 ± 2.9	40 ± 1.0	33 ± 3.0	0 ± 0	39 ± 1.1	13 ± 1.4	0 ± 0	–
10 min NaCl + BSA	62.7 ± 2.5	39.8 ± 0.1	22.7 ± 1.4	0 ± 0	44.1 ± 0.8	0.6 ± 0.4	0 ± 0	0.098 ± 0.12
1 h NaCl + BSA,	63.3 ± 2.7	44.9 ± 0.5	16.1 ± 1.7	0.1 ± 0	44.9 ± 0.5	6.1 ± 0.9	0.2 ± 0	0.07 ± 0.05
24 h NaCl + BSA	73.5 ± 7.2	43.4 ± 2.7	8.0 ± 7.1	0.4 ± 0.6	43.5 ± 2.8	2.4 ± 3.3	4.7 ± 6.6	0.58 ± 0.68
168 h NaCl + BSA	14.7 ± 1.8	45.3 ± 0.6	57.9 ± 1.1	0.1 ± 0	43.9 ± 0.4	28.1 ± 0.1	0 ± 0	1.72 ± 0.24
10 min CA	61.6 ± 9.5	40.9 ± 1.5	16.0 ± 14.0	1.3 ± 1.7	40.8 ± 1.4	6.2 ± 8.3	8 ± 11.4	0.38 ± 0.03
1 h CA	63.0 ± 17.3	41.4 ± 0.6	17.8 ± 22.8	1.5 ± 2.2	40.8 ± 1.8	7.3 ± 10.3	8.3 ± 11.8	0.29 ± 0.19
24 h CA	29.3 ± 8.4	42.0 ± 2.4	44.6 ± 10.8	0.6 ± 0.6	41.5 ± 3.2	22.2 ± 5.6	0.6 ± 1.3	1.91 ± 0.48
168 h CA	24.9 ± 3.6	44.2 ± 1.0	46.9 ± 3.2	0.6 ± 0.3	44.0 ± 1.1	24.9 ± 2.1	0.1 ± 0.2	3.99 ± 0.98

[a] The water contact angles and surface energy values are shown as average values and standard deviations of 2–4 independent samples, 2 different locations on each sample, and 1–2 measurements on the same location, i.e. 4–16 single measurements. Released iron is shown as the average value and standard deviation of three independent samples, which were measured three times, respectively, i.e. 9 single measurements.

Fig. 4. Amount of iron release into solution measured by means of GF-AAS (a), static water contact angles, and corresponding γ^- values (based on water, formamide, and diiodomethane) calculated using the vOCG method (b), and their correlation for individual coupons (c) of stainless steel grade 304 exposed to citric acid (pH 2.4) for 10 min, 1, 24, and 168 h. The error bars show the standard deviation among four uniquely exposed coupons.

concentrations, as in this study [16]. Similar total released amounts of iron were observed for the two solutions after 168 h, explained by similar total amounts of adsorbed BSA, since the maximum amount of adsorbed BSA is independent of the ionic strength at pH 7.4 [21]. Large deviation among individual coupons observed after 24 h exposure in NaCl + BSA indicates a transition from relatively low to significantly higher released amounts of iron, correlated with increased γ^- polar component values and reduced static contact angles, Figs. 3a–c. High levels of iron release clearly correlated with low contact angles and high γ^- values, Fig. 3c.

The most significant change in terms of surface energy was observed for γ^- after 168 h exposure to NaCl + BSA ($p < 0.01$), while no significant difference was observed for the other exposure times, compared to the freshly polished and aged coupons. γ_{LW} increased slightly (significant, $p < 0.01$, after 1 h and 168 h of exposure) when immersed in NaCl + BSA, Table 4, compared with freshly polished and aged coupons. There was no significant difference for γ^+.

Similar trends were observed for stainless steel exposed to citric acid (pH 2.4), Fig. 4, with increased amounts of released iron and calculated γ^- values (Table 4), and reduced water contact angles with time, Figs. 4a and b. There was also a clear correlation between released amounts of iron and both γ^- values and water contact angles, Fig. 4c. The difference of the polar component γ^- was significant ($p < 0.05$) after 24 and 168 h of exposure to citric acid, compared to freshly polished and aged coupons. Corresponding differences for the γ_{LW} and the γ^+ components were significant ($p < 0.05$) after 1 and 168 h (γ_{LW}), and 168 h (γ^+) of exposure in citric acid, Table 4. The results imply that all surface energy components increase with time, indicating a surface with increasingly amphoteric properties.

The results indicate a layer of citrate that becomes more compact and ordered after approximately 24 h of exposure, when low

contact angles were observed, approaching conditions for a totally wetted carboxylated surface (<10°) [65].

In all, observed findings indicate that the surface energy increases with time and correlates with released amounts of iron.

4. Conclusions

The objective of this study was to elucidate the importance and connection between surface physicochemical characteristics including surface energy and wettability and surface oxide composition with the release of iron from stainless steel surfaces in complexing biological media.

No correlation was observed between the surface oxide composition of stainless steel (grade AISI 304) and calculated surface energies or the wettability for polished, aged surfaces in non-complexing solutions. Instead, the surface contamination (adventitious atmospheric carbon or from cleaning solvents) probably strongly influenced the surface energy of stainless steel. The amount of released iron from stainless steel in solutions containing BSA or citrate (10 mM NaCl + 10 g/L BSA, 5 g/L citric acid) strongly correlated with the measured wettability and calculated surface energy. The surface energy components (γ_{LW}, γ^+, γ^-) increased and the static water contact angles decreased with increased amount of released iron. These observations and the delay in released amounts of iron with time strongly suggest an adsorption-controlled ligand-induced metal release process in the presence of BSA and citrate.

Appendix A. Supplementary data

Supplementary data associated with this article can be found, in the online version, at http://dx.doi.org/10.1016/j.colsurfb.2014.06.066.

References

[1] S. Virtanen, Corros. Rev. 26 (2008) 147.
[2] S. Hood, E. Zottola, Food Control 6 (1995) 9.
[3] H. Ksontini, F. Kachouri, S. El Abed, S. Ibnsouda Koraichi, H. Meftah, H. Latrache, M. Hamdi, J. Adhes. Sci. Technol. 27 (2012) 783.
[4] Y. Hedberg, X. Wang, J. Hedberg, M. Lundin, E. Blomberg, I. Odnevall Wallinder, J. Mater. Sci. Mater. M 24 (2013) 1015.
[5] C.-O.A. Olsson, D. Landolt, Electrochim. Acta 48 (2003) 1093.
[6] C. O'Laoire, B. Timmins, L. Kremer, J.D. Holmes, M.A. Morris, Anal. Lett. 39 (2006) 2255.
[7] B. Elsener, A. Rossi, Mater. Sci. Forum 192–194 (1995) 225.
[8] G. Herting, I. Odnevall Wallinder, C. Leygraf, Corros. Sci. 49 (2007) 103.
[9] I. Milosev, H.-H. Strehblow, J. Biomed. Mater. Res. 52 (2000) 404.
[10] J.E. Castle, J.H. Qiu, Corros. Sci. 29 (1989) 591.
[11] U. Schwertmann, Plant Soil 130 (1991) 1.
[12] R.F. Carbonaro, B.N. Gray, C.F. Whitehead, A.T. Stone, Geochim. Cosmochim. Acta 72 (2008) 3241.
[13] Y. Zhang, N. Kallay, E. Matijevic, Langmuir 1 (1985) 201.
[14] Y. Hedberg, J. Hedberg, Y. Liu, I. Odnevall Wallinder, Biometals 24 (2011) 1099.
[15] M.E. Essington, Soil and Water Chemistry – An Integrative Approach, CRC Press, LLC, Boca Raton, 2004.
[16] J.L. Brash, Q.M. Samak, J. Colloid Interface Sci. 65 (1978) 495.
[17] N. Chandrasekaran, S. Dimartino, C.J. Fee, Chem. Eng. Res. Des. 91 (2013) 1674.
[18] C.J. van Oss, Interfacial Forces in Aqueous Media, 2nd edition, Taylor & Francis Group, LLC, Boca Raton, 2006.
[19] L. Boulané-Petermann, Biofouling 10 (1996) 275.
[20] W. Norde, Macromol. Symp. 103 (1996) 5.
[21] S. Fukuzaki, H. Urano, K. Nagata, J. Ferment. Bioeng. 80 (1995) 6.
[22] C. Exartier, S. Maximovitch, B. Baroux, Corros. Sci. 46 (2004) 1777.
[23] G. Lefèvre, L. Čerović, S. Milonjić, M. Fédoroff, J. Finne, A. Jaubertie, J. Colloid Interface Sci. 337 (2009) 449.
[24] N. Kallay, D. Kovacevic, I. Dedic, V. Tomasic, Corrosion 50 (1994) 598.
[25] K. Takahashi, S. Fukuzaki, Biocontrol Sci. 13 (2008) 9.
[26] M.P. Gispert, A.P. Serro, R. Colaço, B. Saramago, Surf. Interface Anal. 40 (2008) 1529.
[27] S. Omanovic, S.G. Roscoe, Langmuir 15 (1999) 8315.
[28] D.C. Hansen, G.W. Luther, J.H. Waite, J. Colloid Interface Sci. 168 (1994) 206.
[29] W. Wu, R. Giese Jr., C.J. Van Oss, Powder Technol. 89 (1996) 129.
[30] Y. Hedberg, K. Midander, Mater. Lett. 122 (2014) 223.
[31] Y. Hedberg, N. Mazinanian, I. Odnevall Wallinder, Environ. Sci. Process. Impacts 15 (2013) 381.
[32] N. Kallay, Z. Torbic, M. Golic, E. Matijevic, J. Phys. Chem. – US 95 (1991) 7028.
[33] W. Stumm, J.J. Morgan, Aquatic Chemistry: Chemical Equilibria and Rates in Natural Waters, 3rd ed., John Wiley and Sons, New York, 1996.
[34] M. Kosmulski, Chemical Properties of Material Surfaces, Marcel Dekker, Inc., New York, 2001.
[35] E. McCafferty, J.P. Wightman, J. Adhes. Sci. Technol. 13 (1999) 1415.
[36] Q. Fu, T. Wagner, Surf. Sci. Rep. 62 (2007) 431.
[37] A. Stoneham, P. Tasker, J. Phys. Chem. C: Solid State 18 (1985) L543.
[38] C. Van Oss, R. Good, M. Chaudhury, Langmuir 4 (1988) 884.
[39] C.J. Van Oss, M.K. Chaudhury, R.J. Good, Chem. Rev. 88 (1988) 927.
[40] C. Della Volpe, D. Maniglio, S. Siboni, M. Morra, J. Adhes. Sci. Technol. 17 (2003) 1477.
[41] R.J. Good, M.K. Chaudhary, Fundamentals of Adhesion, Plenum Press, New York, 1991.
[42] C. Della Volpe, S. Siboni, J. Adhes. Sci. Technol. 14 (2000) 235.
[43] J. Vogelgesang, J. Hädrich, Accredit. Qual. Assur. 3 (1998) 242.
[44] M. Lundin, Y. Hedberg, T. Jiang, G. Herting, X. Wang, E. Thormann, E. Blomberg, I. Odnevall Wallinder, J. Colloid Interface Sci. 366 (2012) 155.
[45] G. Guillemot, G. Vaca-Medina, H. Martin-Yken, A. Vernhet, P. Schmitz, M. Mercier-Bonin, Colloid Surf. B 49 (2006) 126.
[46] G. Lerebour, S. Cupferman, M.N. Bellon-Fontaine, J. Appl. Microbiol. 97 (2004) 7.
[47] G. Anand, F. Zhang, R.J. Linhardt, G. Belfort, Langmuir 27 (2010) 1830.
[48] S. Flint, J. Brooks, P. Bremer, J. Food Eng. 43 (2000) 235.
[49] M. Mantel, J. Wightman, Surf. Interface Anal. 21 (1994) 595.
[50] M.K. Bernett, W. Zisman, J. Colloid Interface Sci. 28 (1968) 243.
[51] A. Ithurbide, I. Frateur, A. Galtayries, P. Marcus, Electrochim. Acta 53 (2007) 1336.
[52] H. Wu, L. Zhuo, Q. He, X. Liao, B. Shi, Appl. Catal. A: Gen. 366 (2009) 44.
[53] C. Jullien, T. Bénézech, B. Carpentier, V. Lebret, C. Faille, J. Food Eng. 56 (2003) 77.
[54] C. Faille, C. Jullien, F. Fontaine, M.-N. Bellon-Fontaine, C. Slomianny, T. Benezech, Can. J. Microbiol. 48 (2002) 728.
[55] C. Van Oss, Colloid Surf. A 78 (1993) 1.
[56] C. Van Oss, R. Good, M. Chaudhury, J. Protein Chem. 5 (1986) 385.
[57] J. Galván, L. Saldaña, M. Multigner, A. Calzado-Martín, M. Larrea, C. Serra, N. Vilaboa, J. González-Carrasco, J. Mater. Sci. Mater. M 23 (2012) 657.
[58] Y. Okazaki, E. Gotoh, Biomaterials 26 (2005) 11.
[59] S. Virtanen, I. Milosev, E. Gomez-Barrena, R. Trebse, J. Salo, Y.T. Konttinen, Acta Biomater. 4 (2008) 468.
[60] L. Boulange-Petermann, C. Jullien, P. Dubois, T. Benezech, C. Faille, Biofouling 20 (2004) 25.
[61] J. Noh, N. Laycock, W. Gao, D. Wells, Corros. Sci. 42 (2000) 2069.
[62] T.H. Muster, A.K. Neufeld, I.S. Cole, Corros. Sci. 46 (2004) 2337.
[63] W. Norde, J. Lyklema, J. Colloid Interface Sci. 66 (1978) 257.
[64] A.P.V.A. do Serro, A.C. Fernandes, B.d.J.V. Saramago, W. Norde, J. Biomed. Mater. Res. 46 (1999) 376.
[65] C.D. Bain, E.B. Troughton, Y.T. Tao, J. Evall, G.M. Whitesides, R.G. Nuzzo, J. Am. Chem. Soc. 111 (1989) 321.